Area, perimeter, density and entropy of objects generated by deposition of particles [1]

Horacio A. Caruso

Departamento de Hidráulica
Facultad de Ingeniería, Universidad Nacional de La Plata - Argentina
hcaruso@volta.ing.unlp.edu.ar

Josué Núñez

Facultad de Ciencias Astronómicas y Geofísica
Universidad Nacional de La Plata - Argentina
jan@fcaglp.fcaglp.unlp.edu.ar

(*Recebido em 14 de março de 2000*)

Abstract: *Each time a particle is added in order to study growth phenomena with a discrete model, the mass of the object increases and its perimeter changes. This change of perimeter may have different values and signs, depending on the place where the particle is added and on the computational model used. We study these changes of perimeter, for the deposition of particles on a two dimensional euclidean space, starting with a line of seeds and using two types of lattices, one composed of square cells and another one in which the cells are equilateral triangles. Functions relating perimeter, density and entropy with the area are studied. Different types of random walks are considered in a particular fashion through the selection of five different possible directions. The usual procedure to study the way the perimeter of an object varies with its area is by means of the well known power-law function. An alternative method is herein proposed to define a similar approach, but it is based upon the probabilities of the changes of perimeter. No attempt has been made in this study to compare numerical results with those of real phenomena.*

Key words: *random walks, aggregation, ballistic aggregation, fractal dimension, growth of objects*

[1]This work was partially supported by the Departamento de Hidráulica, Facultad de Ingeniería, Universidad Nacional de La Plata; CONICET (Consejo Nacional de Investigaciones Científicas y Técnicas); and Facultad de Ciencias Astronómicas y Geofísica, Universidad Nacional de La Plata, Argentina.

Resumo:*Sempre que se acrescenta uma partícula para estudar fenômenos de crescimento, a massa do objeto cresce e seu perímetro muda. Essa mudança de perímetro pode ter valores de sinais diferentes, dependendo do lugar onde a partícula é adicionada e do modelo computacional usado. Estudam-se essas mudanças de perímetro para deposições de partículas num espaço euclidiano de dimensão 2, partindo de uma linha de sementes e usando dois tipos de redes, uma composta de células quadradas e outra em que as células são triângulos equiláteros. Estudam-se funções que relacionam perímetro, densidade e entropia com a área. Diferentes tipos de percursos aleatórios são considerados de uma maneira particular através de uma escolha de cinco possíveis direções diferentes. O processo usual para estudar como o perímetro de um objeto varia com a sua área é pela bem conhecida lei da potência. Propõe-se um método alternativo para definir um enfoque semelhante, porém baseado nas probabilidades de mudança de perímetro. Não se faz nenhuma comparação numérica com resultados associados aos fenômenos reais.*

Palavras-chave: *percursos aleatórios; agregação; agregação balística; dimensão fractal; crescimento de objetos*

1 Introduction

The study of growth phenomena has concentrated the attention of scientists in recent years [1], both in theory and its applications. The results and conclusions from models are giving answers to the complex behavior of some natural processes. According to Meakin [2,3], "One of the most important models which generates fractal structures is the Witten-Sander model [4] for diffusion-limited aggregation". From this early contribution a wide variety of phenomena has been studied, for example, purification of air and water [5-7], particles or atoms added to surfaces and fibers [8-11], colloids and coagulated aerosols [12,13], chemical species precipitation from supersaturated matrix and crystal growth from a superheated melt [14], formation of dust, soot and dendrites, polymer gelation [15-18], percolation [19-25], critical phenomena [26], sol-gel transition [27], early stages of nucleation [28], dendritic crystal growth, the coagulation of smoke particles [29], red blood cell aggregation [30], dielectric breakdown [31], fluid-fluid displacement in Hele-shaw cells and porous media [32], electrodeposition [33,34], the formation of sputter-deposited thin films [33], biological processes, a variety of pattern formation processes and theoretical works [31,35-56].

One of the models which appears to be the simplest (if only its rules and initial conditions are contemplated), consists of a seed, or a line of seeds, implanted at the bottom of a region; the growth process starts by releasing a particle from the top of the region and, due to some force field, it falls down until it reaches a site adjacent to a seed or to an already deposited particle; at this instant it is considered a permanent part of the cluster. The process continues by throwing another particle.

The region where deposition takes place is herein composed of cells of two different shapes: triangular and square cells. The study is performed taking into account that, each time one cell is added, the area increases and the perimeter changes. Thus,

variables are considered in a 'microscopic' fashion (the size of the cells) and an instantaneous picture of deposition is obtained, allowing the study of local changes of perimeter.

The first part of the present paper deals with the problem of pure vertical fall of particles (ballistic deposition, where diffusion is absent); in the second part particles perform a random walk (diffusion-controlled deposition).

2 Description of the numerical model and definitions

2.1 Square and triangular lattices

We shall perform numerical experiments of deposition on two different types of lattices, one composed of square cells and another with equilateral triangles, as shown in Figure 1(a) and 1(b), respectively. The sides of the squares and triangles have a length equal to unity. Thus, the area of each square is equal to unity, while the area of each triangle is $\sqrt{3}/4$.

The region where deposition takes place has a total of J_F cells along the horizontal (each cell defined by a *J-index)* and K_F cells along the vertical (with *K-index* identifying each row of cells). The region is assumed to be cylindrical in shape; thus, a periodic boundary condition is set in the horizontal direction. For this reason the vertical limits of the space have a zigzag course in the triangular lattice.

2.2 Definition of a density

Figure 1(a) shows an assumed example of deposition on a square lattice; column $J = 6$ has 4 filled cells and 2 empty cells in between. The density ρ_J of this particular column shall be defined as

$$\rho_J = \rho_6 = 4/\left(4+2\right) \tag{1}$$

The empty cells are in the "shadow" of a filled one. If the procedure is extended to all columns, then the density ρ of the object shall have the expression

$$\rho = \sum_{J=1}^{J_F} \rho_J \tag{2}$$

As an example, Figure 1(a) has 23 filled squares and 11 empty ones. The density of objects generated on a triangular lattice is defined in a similar fashion. The example of Figure 1(b) has 45 filled triangles and 16 empty ones in the shadow of filled triangles. Notice that column $J = 9$ has 3 filled cells and an equal amount of empty triangles, while column $J = 14$ has no empty triangles in the shadow of filled ones.

Clusters generated by deposition contain empty channels (fiords), opened to the exterior, and porous regions trapped by filled cells. A better definition of density should contain this information, but its programming on a computer seems to be

rather involved for the moment specially due to computer memory limitations. The previous definition of density, however, provides good information in all of our objects and is very simple to calculate.

The numerical model herein used calculates the maximum height reached by the object each time a new particle is deposited, but it was found that this variable does not add important information about the behavior or deposition. If a mean maximum height is considered of import, it may be easily computed from the results herein presented, with the product of the density multiplied by the area and divided by J_F.

2.3 Changes of area and perimeter

Each time a particle finds an empty site, for any type of growth model (diffusion-limited aggregation, model of Eden, ballistic deposition, etc.), the area of the object changes with an amount given by

$$\Delta A = A_{n+1} - A_n \tag{3}$$

when one particle is aggregated; in the above equation, A_n and A_{n+1} are, respectively, the areas before and after the aggregation of one particle takes place. The quantity ΔA shall always be considered positive, i.e., the cell is permanently incorporated into the cluster.

Accordingly, each time the area increases with ΔA, then the perimeter changes as

$$\Delta P = P_{n+1} - P_n \tag{4}$$

where P_n and P_{n+1} are, respectively, the perimeters before and after one particle has been aggregated.

For the square lattice of Figure 1(a), ΔP may have only 5 different values: $\Delta P = +4$ belongs to a particle added to the vertex of an already existing particle; $\Delta P = +2$ comes from the addition of a cell to the side of another filled cell; $\Delta P = 0$ is the result of particles aggregated at the empty corner formed by two previously added particles; $\Delta P = -2$ pertains to a cell deposited at the slot formed by 3 already deposited cells; and finally, $\Delta P = -4$ shall be the result of a particle added to a site surrounded by 4 filled cells. Examples of all possible events are annotated in Figure 1 (a). It should be noticed that a lattice composed of hexagons has the same values for the changes of perimeter mentioned in the paragraph above.

The possibilities of ΔP for the triangular lattice, if compared with the square lattice, are reduced from 5 to 4, and have the following values: $\Delta P = +3$ is produced when a triangle is deposited at the vertex of a filled triangle; $\Delta P = +1$ comes from the event that a cell is attached to the side of a previously filled cell; $\Delta P = -1$ is the result of a triangle added at the wedge between two filled triangles; and finally, $\Delta P = -3$ comes from the occupation of a free site trapped between 3 filled triangles. All these cases are shown in Figure 1 (b).

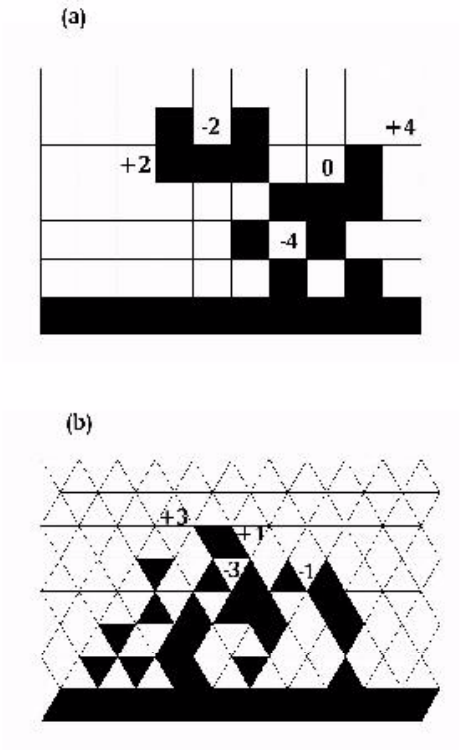

Figure 1. Two examples of small clusters generated by deposition, (a) with a lattice composed of square cells and (b) with triangular cells. Both types of cells have their sides equal to unit; thus, the area, ΔA, of each square is equal to unity, while that of the triangle is $\sqrt{3}/4$. Deposition takes place in a region composed of J_F cells in the horizontal and K_F cells in the vertical direction. There is a line of seeds placed at the bottom of the region in order to start the growth of the object. Each time the area increases with ΔA the perimeter changes with ΔP. The different changes of perimeter (ΔP_k), for each lattice, are indicated with numbers in the empty cell it would occupy if allowed to be deposited there. For the triangular lattice there are only four possible changes of perimeter, while for the square lattice there are five.

If the possibilities of $\Delta P = +4$ for the square lattice, or $\Delta P = +3$ for the triangular lattice, are set to zero as an initial condition, it means that the growth model does not allow particles to be deposited at the vertex of already existing sites. This criteria reduce the number of variables (degrees of freedom) participating in the problem.

2.4 Probabilities of the changes of perimeter

If the changes of perimeter are recorded each time a particle is deposited, then a statistical study of the probabilities, $p(\Delta P_k)$, may be performed; they are given by

$$p(\Delta P_k) = \frac{n_k}{n_f} \tag{5}$$

where n_k is the number of cases found with a given ΔP_k, and n_f is the total amount of particles added. Probabilities

$$\{p(\Delta P_k)\}_{\Delta P_k=-4,-2,0,+2,+4} \tag{6}$$

$$\{p(\Delta P_k)\}_{\Delta P_k=-3,-1,+1,+3} \tag{7}$$

for the square and triangular lattices, respectively, give good information about the available sites where a cell may be deposited as the object grows. In the following paragraphs it shall be seen that they may also be of interest in the study of the behavior of all growth phenomena.

2.5 Information entropy

Let us consider a manifold P provided with a normalized measured p. Let $\Delta P = \{\Delta P_i\}_{i=1,\ldots,n} \subset P$; then we can define an entropy [57] of the set ΔP as

$$S(\Delta P) = -\sum_{i=1}^{n} p(\Delta P_i) \ln\left(p(\Delta P_i)\right) \tag{8}$$

where ΔP is the set of all possible changes of the perimeter, and the measured p is the probability associated with these changes. The above values of the probabilities of the different types of changes of perimeter may be used to compute the information entropy of the system, relative to the maximum disorder (given by k_f possible events), by means of

$$S = \frac{\sum_{k=1}^{k_f} p(\Delta P_k) \ln\left(p(\Delta P_k)\right)}{\ln(1/k_f)} \tag{9}$$

with $k_f = 5$, for the square, and $k_f = 4$ for the triangular lattice, respectively. The value of k_f may be smaller if a particular ΔP_k is initially set to zero.

2.6 Anisotropic random walk

In the general case of deposition a particle starts its way from the upper part of the lattice and falls down, performing a random walk; the intention of the particle is to reach a cell which is empty and in the vicinity of an already filled cell. The random walk is herein performed by the choice of one of the 5 different possibilities:

$$D(I) \text{ for } I = 1 \text{ to } 5 \tag{10}$$

defined in Figure 2, with the condition

$$\sum_{I=1}^{5} D(I) = 1 \tag{11}$$

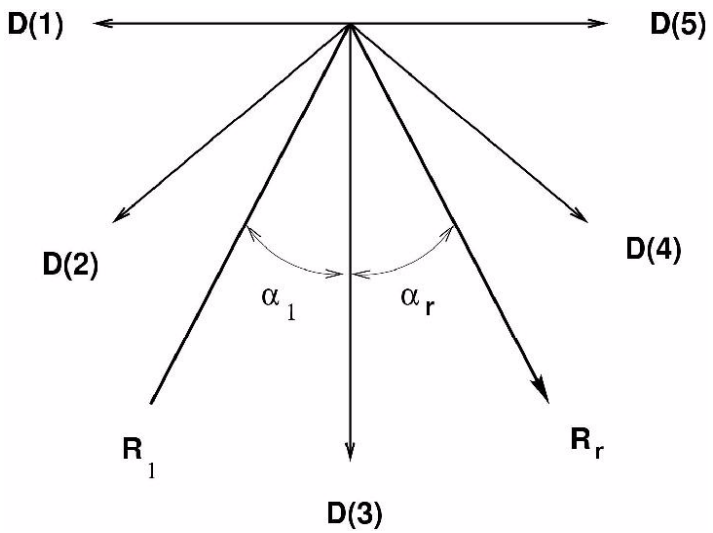

Figure 2. The definition of the random walker used in this paper to grow objects; it may select one from the five different directions, $D(I)$, for $I = 1$ to 5. The sum of all these possibilities is equal to unity. If $D(3) = 1$, then the direction of fall is always along the vertical; if any of the other possible directions $D(I)$ is different from zero the random walker shall perform lateral steps. In the present paper we shall consider symmetrical objects only; this is achieved by setting the initial conditions: $D(1) = D(5)$ and $D(2) = D(4)$. Otherwise, the columnar structure of the object shall be inclined with respect to the vertical. Directions $D(1)$, $D(2)$ and $D(3)$ have a resultant R_l inclined with an angle α_l to the left; similarly, $D(3)$, $D(4)$ and $D(5)$, inclined to the right. Due to the conditions of symmetry, the different types of random walks may be characterized by a modulus of intrusion (R) and by an angle of diffusion (α).

If a particle is in position (J, K) in the lattice and the choice is direction $D(1)$, then it shall occupy the cell identified by $(J-1, K)$; if the chosen direction is $D(2)$ it shall fall in the position $(J-1, K-1)$; if it performs a vertical down step with the possibility $D(3)$ the name of the cell shall be $(J, K-1)$; if the possibility $D(4)$ is randomly chosen the walker shall go to position $(J+1, K-1)$; and finally, if a step to the right is chosen by means of $D(5)$ the walker shall reach the cell $(J+1, K)$. An initial condition given by $D(3) = 1$ shall result in a pure vertical fall of particles; the condition $D(1) = D(5) = 0.5$ is avoided since it does not allow particles to make a single step downwards.

The initial conditions

$$D(1) = D(5) \text{ and } D(2) = D(4) \tag{12}$$

shall produce a symmetrical object; otherwise, the columnar structure of the object shall be inclined with respect to the vertical; see for instance [1], page 155.

A random walk defined as in Figure 2 has 4 independent variables; in order to treat the walker in a simpler fashion we shall assume that $D(1), D(2)$ and $D(3)$ are

"vectors", the resultant of which have an argument α_l and a modulus R_l, to the left of the vertical; similarly, the resultant of $D(3), D(4)$ and $D(5)$ have an argument α_r and a modulus R_r, to the right. The previous conditions of symmetry in Eq.(2.12) are replaced by

$$\alpha = \alpha_l = \alpha_r \text{ and } R = R_l = R_r \tag{13}$$

Thus, a random walk resulting in a symmetrical object shall be defined by 2 variables only: and "angle of diffusion" (α) and a "modulus of intrusion" (R).

For a given pair, (R, α), and for a symmetrical object, the possibilities $D(I)$ of a random walk are given through the solution of the system of equations

$$2D(1) + 2D(2) + D(3) = 1 \tag{14}$$

$$D(1) + \frac{\sqrt{2}}{2}D(2) = R\sin\alpha \tag{15}$$

$$\frac{\sqrt{2}}{2}D(2) + D(3) = R\cos\alpha \tag{16}$$

For a given α the modulus of intrusion varies in the range

$$R_{\min} \leq R \leq R_{\max} \tag{17}$$

where

$$R_{\min} = \frac{1}{2\sin\alpha + \cos\alpha}, \text{ for } 0 \leq \alpha \leq \frac{\pi}{2} \tag{18}$$

The maximum modulus of intrusion is given by

$$R_{\max} = \frac{1}{(2\sqrt{2}-1)\sin\alpha + \cos\alpha}, \text{ for } 0 \leq \alpha \leq \frac{\pi}{4} \tag{19}$$

and by

$$R_{\max} = \frac{1}{2\sin\alpha + 2(\sqrt{2}-1)\cos\alpha}, \text{ for } \frac{\pi}{4} \leq \alpha \leq \frac{\pi}{2} \tag{20}$$

A pure vertical fall is given by $R_{\min} = R_{\max} = 1$ and $\alpha = 0$. For any other angle of diffusion ($\alpha > 0$), there shall be a difference between $R_{\max}$ and $R_{\min}$.

The maximum difference between $R_{\max}$ and $R_{\min}$ corresponds to $\alpha = \pi/4$. In this case, $R_{\max} = 0.5$ with $D(1) = D(5) = D(3) = 0$ and $D(2) = D(4) = 0.5$. The minimum value of the modulus of intrusion is $R_{\min} = 0.471406$, with $D(1) = D(5) = D(3) = 1/3$ and $D(2) = D(4) = 0$. This maximum difference, $R_{\max} - R_{\min} = 0.5 - 0.47 = 0.03$, seems to be rather small, but it shall be seen that the different types of random walks play a very important role upon densities, entropies, changes of perimeter and probabilities of changes of perimeter. It seems to the authors that all numerical models of growth phenomena worked out in the past have considered $D(I) = 1/5$, for $I = 1$ to 5, and some of them, perhaps, with $D(I) = 1/8$, for $I = 1$ to 8.

2.7 How and when a particle is deposited

At a certain stage *(n)* of growth, the particle which is to be deposited at $n+1$ starts its random walk at a horizontal position chosen at random between $J = 1$ and $J = J_F$, and at vertical position (K-index) which is 5 cells above the highest reached during stage n. The particle starts its random walk following the prescriptions given by the 5 possible directions described in Figure 2. If the particle reaches an empty cell and has an adjacent filled cell the program makes a halt. It computes the change of perimeter ΔP would the particle be deposited in the empty cell. If the change of perimeter is allowed then the particle is considered to be permanently deposited in the empty site. If ΔP is not allowed the particle is "killed" and a new random walk starts in the manner previously described.

We shall only consider symmetrical objects in the present study. Thus, random walks are restricted to the conditions given by Eqs.(2.12) or (2.13). In order to start deposition, a line of seeds is placed at the bottom of the region, i.e., at $K = 1$, from $J = 1$ to $J = J_F$. No particles are allowed to be deposited at the vertices of already existing particles. In consequence, the only possibilities of changes of perimeter shall be

$$p(-2), \quad p(0) \quad \text{and} \quad p(+2) \tag{21}$$

for the square lattice, and

$$p(-3), \quad p(-1) \quad \text{and} \quad p(+1) \tag{22}$$

for the triangular lattice. Then, $k_f = 3$ in Eq. (2.9).

3 A new approach for the study of growth phenomena

The usual procedure to study fractal [58] growth phenomena is by means of the well known power-law function

$$A = f_f \, P^D \tag{23}$$

which relates the area of the object and its perimeter by means of a form factor (f_f) and the fractal dimension (D).

Let us assume we have performed an experiment of deposition (or aggregation) in which the measures, $p(\Delta P_k)$, are available [59]. We define the mapping by

$$A_{n+1} \quad = A_n + \Delta A \tag{24}$$

$$P_{n+1} \quad = P_n + \langle \, \Delta P \, \rangle_{A_n} \tag{25}$$

where

$$\langle \Delta P \rangle_{A_n} = \int_P \Delta P \; p \, (\Delta P, A_n) \; d\Delta P \tag{26}$$

and $p \, (\Delta P, A_n)$ is the evolution of $p \, (\Delta P)$ with respect to the area at iteration n.

For the case of numerical models of growth in which there is a finite number (k_f) of increments of perimeter, then the expectation value is

$$\langle \Delta P \rangle_{A_n} = \sum_{k=1}^{k_f} \Delta P_k \, p\,(\Delta P_k) \tag{27}$$

Rewriting Eqs. (3.2) and (3.3) as:

$$\delta A = \Delta A \tag{28}$$

$$\delta P = \langle \Delta P \rangle_{A_n} \tag{29}$$

we can define the incremental form for the evolution of the system by

$$\frac{\delta P}{\delta A} = \frac{\langle \Delta P \rangle_A}{\Delta A} \tag{30}$$

Integrating over all the range of variation of A, we find that

$$P - P_1 = \frac{1}{\Delta A} \int_{A_1}^{A} \langle \Delta P \rangle_A \, \delta A \tag{31}$$

We can see from Eq. (3.9) that the perimeter is a function of the area, i.e., it is an inverse form of Eq. (3.1). This behavior comes from the dependence of the probabilities on the area. A trivial case occurs when the probabilities are constant, i.e., $\langle \Delta P \rangle_A = \langle \Delta P \rangle$; then

$$P = \frac{\langle \Delta P \rangle}{\Delta A} A \tag{32}$$

This simple example shows that the fractal dimension, when the probabilities remain unchanged, is equal to unity; furthermore, it is found that the form factor has the new meaning

$$f_f = \frac{\Delta A}{\langle \Delta P \rangle} \tag{33}$$

A non-trivial dependence of the perimeter on the area, for an object generated with any growth model, may be obtained by assuming that the quantities $p\,(\Delta P_k)$ are given by functions of the type

$$p\,(\Delta P_k, A) = p_1\,(\Delta P_k) + g\,(\Delta P_k)\ A \tag{34}$$

The gradients are expressed by

$$g\,(\Delta P_k) = [p_f\,(\Delta P_k) - p_1(\Delta P_k)]/(A_f - A_1) \tag{35}$$

where $p_1(\Delta P_k)$ are initial probabilities, and $p_f\,(\Delta P_k)$ are final probabilities, when the areas are A_1 and A_f, respectively.

If we define

$$K_1 = \frac{1}{\Delta A} \sum_{k=1}^{k_f} \Delta P_k \, p\,(\Delta P_k) \tag{36}$$

and

$$K_2 = \frac{1}{2\Delta A} \sum_{k=1}^{k_f} \Delta P_k \, g\,(\Delta P_k) \tag{37}$$

then

$$P = P_\imath + K_1(A - A_\imath) + K_2(A^2 - A_\imath^2) \tag{38}$$

In other words, the previous equation expresses the important fact that, when the probabilities of changes of perimeter do not change with the area, then the perimeter varies linearly with the area. When the probabilities of changes of perimeter vary linearly with the area, then the perimeter varies with the second power of the area. We shall return to these matters on later chapters.

In order to see if the theoretical solution given by Eq. (3.16) satisfies the algorithm expressed by Eqs. (3.2) and (3.3), if the increments of perimeter ΔP are given by an expression of the type of Eq. (3.12), a very simple numerical model may be developed. The results are quite satisfactory, provided the number of steps of integration (number of increments ΔA) are of the order of 100000. Several types of probabilities were tested for Eq. (3.12), even an oscillatory one; in this particular case, if the frequencies of oscillation are relatively high, the number of steps should exceed 500000.

In brief, for a function $Y = f(X)$ generated with $\Delta Y = \textit{constant}$ and with ΔX chosen at random, a theoretical solution is derived, and this solution reproduces the function surprisingly well.

4 Experimental results

4.1 Numerical experiments with vertical fall of particles

A large number of numerical experiments were performed, each one with an object sufficiently large to yield significant results and, at the same time, small enough to be compatible with our computing facilities. There was a first group of experiments with the square lattice and a second one with the triangular lattice, both for a pure vertical fall of particles. Due to the disposition of cells, the width of the object for the square lattice is $W = J_F$, while that of the triangular lattice is $W = J_F/2 + 0.5$.

Three different lines of seeds (number of cells placed at the bottom of the region) were studied, namely, $J_F = 100, 500$ and 1000. Clusters were generated with a maximum area, $A_{\max}$, of the order of 141000, 704000 and 1404000, respectively, for the square lattice. The maximum area was of the order of 81200, 403400 and 806300, respectively, for triangles. Deposition continued until the object reached an approximate maximum height of 2000 units.

For each J_F, 30 different objects were generated, each one with different series of random number. (The random number generator comes from a subroutine developed by D. Carpintero [60]). The following variables were recorded: area, perimeter, maximum height, density, entropy, $p(\Delta P_k)$, and the two constants of the power-law function of Eq. (3.1).

All variables studied (and their standard deviations) indicate that at the beginning of growth there is a short transient state with a relatively large dispersion of results, but very soon, when the area increases, this dispersion is strongly attenuated.

Let us consider, as an example, objects with $J_F = 100$, treated with a square lattice. When the area is very small, between the limits $8000 \leq A \leq 16000$, the mean density (of the 30 different numerical experiments) is $\rho = 0.48769$ with a standard deviation of ± 0.00081; with a larger size, for $64000 \leq A \leq 72000$, the mean density is $\rho = 0.47641 \pm 0.00004$; at the end of the experiments, when the cluster are largest, with $118000 \leq A \leq 136000$, the mean density is $\rho = 0.47476 \pm 0.00001$, similar to the previous one.

It has been observed, through 30 numerical experiments, each with a different series of random numbers, each for three different lines of seeds at the bottom, ($J_F = 100, 500$ and 1000), and all of them for both a square and a triangular lattice, that densities, entropies and probabilities of the different changes of perimeter are nearly the same if they are measured at the maximum area, $A_{\max}$, or at half of it, $A_{\max}/2$. This assures that the transient state has ended when the variables of the present paper are studied, at $A_{\max}$.

Let us concentrate our attention now on the final probabilities of the different changes of perimeter, $p(\Delta P_k)$, when the area is $A_{\max}$. Numerical results, shown in Table 1, clearly indicate that they are independent of the width, J_F, of the object, for both types of lattices.

Probabilities $p(+2)$ with $\Delta P = +2$ for squares, and probabilities $p(+1)$ with $\Delta P = +1$ for triangles, are by far the highest of all possible changes of perimeter. This means that the object generated by deposition offers many places at the sides of already existing cells. Probabilities $p(0)$ and $p(-1)$, for squares and triangles, respectively, are smaller than the previous ones; the smallest probabilities are $p(-2)$ and $p(-3)$, for squares and triangles, respectively. It may be seen that, for the square lattice

$$p(+2)/p(0) = 4.7 \quad \text{and} \quad p(+2)/p(-2) = 37$$

while for the triangular lattice

$$p(+1)/p(-1) = 5.3 \quad \text{and} \quad p(+1)/p(-3) = 210$$

It should be pointed out that these results belong to a pure vertical fall of particles; for other types of random walks, $p(-2)$ and $p(-3)$ may become negligible, or zero. This conclusion may be of interest for a theoretical study of deposition.

If we use the subscript *'t'* for the triangular lattice and *'s'* for the square one, the ratio of densities is $\rho_t/\rho_s = 1.324$, for $J_F = 100, 500$ and 1000. One interesting conclusion from these results is that the densities of objects studied with a triangular

lattice are always greater than those for the square, and that they are independent of the form of the region of deposition (very narrow or wide).

Square Lattice	Triangular Lattice
$J_F = 100$	
$p(-2) = 0.02166$	$p(-3) = 0.00387$
$p(0) = 0.17121$	$p(-1) = 0.15804$
$p(+2) = 0.80710$	$p(+1) = 0.83809$
$J_F = 500$	
$p(-2) = 0.02187$	$p(-3) = 0.00396$
$p(0) = 0.17330$	$p(-1) = 0.15900$
$p(+2) = 0.80679$	$p(+1) = 0.83704$
$J_F = 1000$	
$p(-2) = 0.02191$	$p(-3) = 0.00398$
$p(0) = 0.17158$	$p(-1) = 0.15918$
$p(+2) = 0.80651$	$p(+1) = 0.83684$

Table 1: Probabilities ($p(\Delta P_k)$) of the different changes of perimeter (ΔP_k), for different amounts of particles (J_F), placed at the bottom of the region as seeds, in order to start deposition. With the initial restriction that no particles are allowed to be added at the vertices of already deposited particles, the probabilities for the square lattice are $p(-2)$, $p(0)$ and $p(+2)$, while for the triangular lattice they are $p(-3)$, $p(-1)$ and $p(+1)$. It may be seen that an increase in J_F does not change the probabilities $p(\Delta P_k)$ in a significant fashion.

The area of a square circumscribed in a circle is A_{sq}; the area of an hexagon composed of six equilateral triangles and circumscribed in the same circle is A_{hex}. The ratio of both areas is $A_{hex}/A_{sq} = 2.25/\sqrt{3} = 1.299$. The similitude between 1.32 and 1.30 does not seen to be just a mere coincidence.

If we turn our attention to entropies S, with both triangular (subscript *'t'*) and square lattices (subscript *'s'*), for $J_F = 100, 500$ and 1000, we see that the former is lower than the latter, and that the ratio, $S_t/S_s = 0.828$, remains approximately constant, also no matter how narrow or how wide the region is. Deposition of triangles leads to objects with more order than those made of squares.

In order to compute the form factor (f_f) and the fractal dimension *(D)* of Eq. (3.1), areas were considered in different ranges, in order to see the influence of the transient state of deposition. A brief summary of results is in Table 2.

Triangular lattice

J_F	Range of areas	f_f	D
100	$20000 \leq A \leq 81017$	0.6535	0.9992
100	$70000 \leq A \leq 81017$	0.6439	1.0000
500	$200000 \leq A \leq 403351$	0.6556	0.9994
500	$300000 \leq A \leq 403351$	0.6524	0.9997
1000	$400000 \leq A \leq 806270$	0.6636	0.9986
1000	$600000 \leq A \leq 806270$	0.6625	0.9987

Square lattice

J_F	Range of areas	f_f	D
100	$72000 \leq A \leq 141000$	0.6457	0.9989
100	$128000 \leq A \leq 141000$	0.6557	0.9976
500	$350000 \leq A \leq 704000$	0.6476	0.9988
500	$600000 \leq A \leq 704000$	0.6465	0.9990
1000	$700000 \leq A \leq 1404000$	0.6437	0.9993
1000	$1200000 \leq A \leq 1404000$	0.6384	0.9999

Table 2: From the results of numerical experiments for the area A and the perimeter P of ballistic objects, for different sizes J_F and for the two types of lattices herein studied, the form factor (f_f) and the fractal dimension (D), for the power-law function $A = f_f P^D$ has been determined by a least-square method. The computations are performed for different ranges of the area in order to show that a stable growth has been reached. It may be appreciated that the fractal dimension is very close to unity. See the contents of the text for a new interpretation of the form factor relating it with the sum of products $\Delta P_k \, p(\Delta P_k)$.

4.2 The form factor seen from two points of view

In Table 2, for the triangular lattice (with $\Delta A = \sqrt{3}/4$), for $J_F = 100, 500$ and 1000, and for the highest ranges of areas, the form factors f_f obtained were

$$0.6439, \quad 0.6524 \quad \text{and} \quad 0.6625$$

respectively. From Eqs. (3.5) and (3.11), the form factor is

$$f_f = \frac{\Delta A}{[-3p(-3) - p(-1) + p(+1)]} \tag{39}$$

If the results of Table 1 are used with the previous equation, the following form factors are obtained:

$$0.6478, \quad 0.6500 \quad \text{and} \quad 0.6504$$

If the results for the square lattice, also in Table 2, (with $\Delta A = 1$), are compared in the same fashion, it may be seen that for the least-square curve fitting the form factors are given by

$$0.6557, \quad 0.6465 \quad \text{and} \quad 0.6384$$

while from Table 1 and with the new method of the probabilities of changes of perimeter, using

$$f_f = \frac{\Delta A}{[-2p(-2) + 2p(+2)]} \tag{40}$$

the results of numerical experiments yield

$$0.6366, \quad 0.6370 \quad \text{and} \quad 0.6373$$

The comparison of results seems to be reasonable good, if it is taken into account that they come from two entirely different methods. One of the methods (Table 2) comes from the classical curve fitting of the area as a function of the perimeter. The other comes from the theoretical results of Eqs. (3.5) and (3.11).

The form factor was generally regarded as a variable which supposedly reflected the form of the object. However, the results of the present paper suggest that it should be considered as an indication of the behavior of a new variable, namely, the sum of the products of the changes of perimeter multiplied by their respective probabilities, i.e. the sum of $\Delta P_k \, p(\Delta P_k)$, the expectation value.

4.3 Non-vertical fall of particles

When particles fall with a pure vertical direction, i.e., when $D(3) = 1$ or $\alpha = 0$, there is no possibility for a particle to be deposited below an already added cell, for a particular column. This means that no particle shall be incorporated in the shadow (columnwise) of another one. When the random walker is allowed to make lateral steps ($\alpha > 0$) some particles may reach the interior of the object. Nevertheless, the total amount of particles added inside the object is overwhelmingly small, if compared with the total number of cells added, and it increases with α and R. For instance, for $\alpha = 45^0$ and $R = R_{\min} = 0.4714$ one numerical experiment showed that 23 cells found an available site below a higher cell in the same column, when the object contained 117000 cells; the intruders are a small fraction of the total area, namely, 0.02 %. Another experiment, for $\alpha = 85^0$ and $R = R_{\min} = 0.4809$, showed that there were 363 particles, out of a total of 59000, (0.6 %) added in the inside of different columns. Similar results were repeated in several experiments, and, though isolated examples, they show that the vast majority of particles reach the 'surface' of the object (the highest cell for each column). Particles incorporated into the interior of the object are rare, even for angles of diffusion very close to $\pi/2$.

The highest densities and entropies are obtained when particles fall vertically. When the chances of a lateral step for the falling particles are different from zero the object decreases its density and its entropy. In order to show this phenomenon a series of numerical experiments were performed with triangular and square lattices,

and for angles of diffusion ranging from $\alpha = 0$ up to $\alpha = 84^o$, with increments of 2^o; three values of the modulus of intrusion were chosen: $R = R_{\min}$, $R = R_{\text{med}} = (R_{\min} + R_{\max})/2$ and $R = R_{\max}$;the dimensions of the lattices were $J_F = K_F = 500$. The total of 258 experiments are shown in Figure 3. The results near the maximum densities and entropies are those for the smallest angles of diffusion; those far from these maxima correspond to angles approaching $\pi/2$.

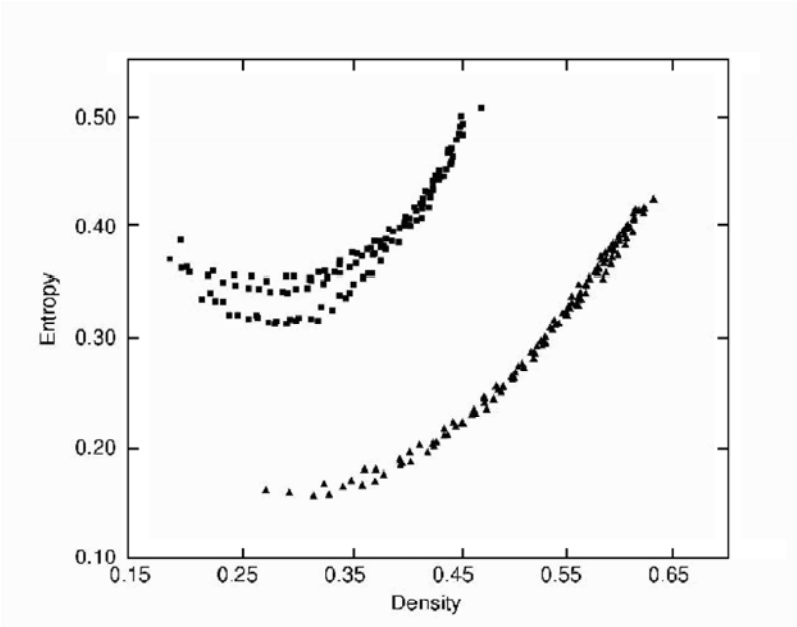

Figure 3. Entropy as a function of density for the square lattice (upper group of results) and triangular lattice (lower group). The numerical experiments start with $\alpha = 0^o$ and $R = 1$, which is equivalent to say that $D(3) = 1$ and $D(1) = D(2) = D(4) = D(5) = 0$. These random walkers yield maximum density and maximum entropy. The rest of results are obtained in the range $0^o < \alpha \leq 84^o$, increasing the angle by 2^o. For each angle, three different modulus of intrusion are used: $R = R_{\min}$, $R = R_{\text{med}} = (R_{\min} + R_{\max})/2$ and $R = R_{\max}$.

Those values of the highest α, which are responsible for the lowest densities, should be taken with caution; many more experiments, with the same initial conditions but with different series of random numbers and much larger sizes of the lattices, should have been performed. These experiments are too costly for the authors at the present moment due to limitations in computer facilities. However, it may be clearly seen that there are objects with constant entropy and different densities, and that these differences of densities increase when the angle of diffusion increases. When the objects behave in a more orderly fashion (low entropies) they exhibit a wider variety of densities. The other point of view is obviously true: a constant density may result in objects with different indices of chaoticity. Through the observation of experimental results it is found that the lowest densities ($\rho_{\min}$)

and entropies ($S_{\min}$) result from the minimum modulus of intrusion ($R_{\min}$); the maximum densities ($\rho_{\max}$) and entropies ($S_{\max}$) are due to the maximum modulus ($R_{\max}$). This fact is not clear from Figure 3. In order to emphasize this phenomenon a series of numerical experiments were performed with triangular and square lattices, and for angles of diffusion $\alpha = 10^o$, 45^o and 85^o;the modulus of intrusion varied between $R_{\min}$ and $R_{\max}$ according with Eqs. (2.18), (2.19) and (2.20).The region where deposition takes place has the dimensions: $J_F = K_F = 500$.

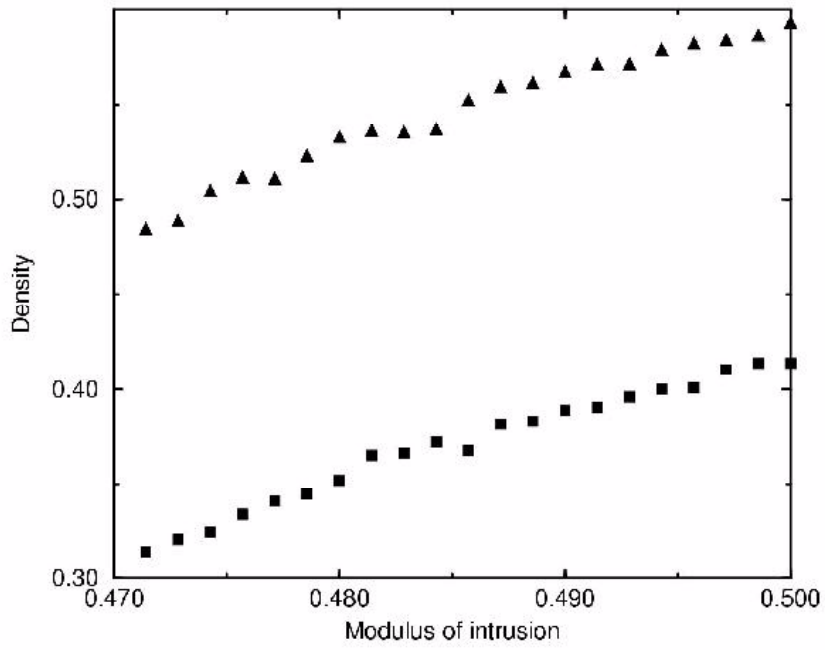

Figure 4. Density as a function of the modulus of intrusion, for the range $R_{\min} \leq R_{\max}$, for triangular and square lattices, with an angle of diffusion $\alpha = 45^o$. The purpose of this figure is to show the increase of density due to an increase of the modulus of intrusion. For $R = R_{\min}$, then $D(1) = D(3) = D(5) = 1/3$ and $D(2) = D(4) = 0$; for $R = R_{\max}$, then $D(2) = D(4) = 1/2$ and $D(1) = D(3) = D(5) = 0$.

The changes of densities due to changes of the modulus of intrusion are shown in Figure 4, for an angle of diffusion $\alpha = 45^o$, for squares and triangles. Now it is evident that there is an increase of density, $\Delta\rho = \rho_{\max} - \rho_{\min}$ when the modulus increases from $R_{\min}$ to $R_{\max}$; $\Delta\rho = 0.587 - 0.485 = 0.102$ for the triangular lattice, and $\Delta\rho = 0.413 - 0.314 = 0.099$ for squares. Concerning entropies, shown in Figure 5, the objects herein studied follow the same behavior: $\Delta S = S_{\max} - S_{\min} = 0.360 - 0.239 = 0.121$ for triangles and $\Delta S = 0.407 - 0.320 = 0.087$ for squares.

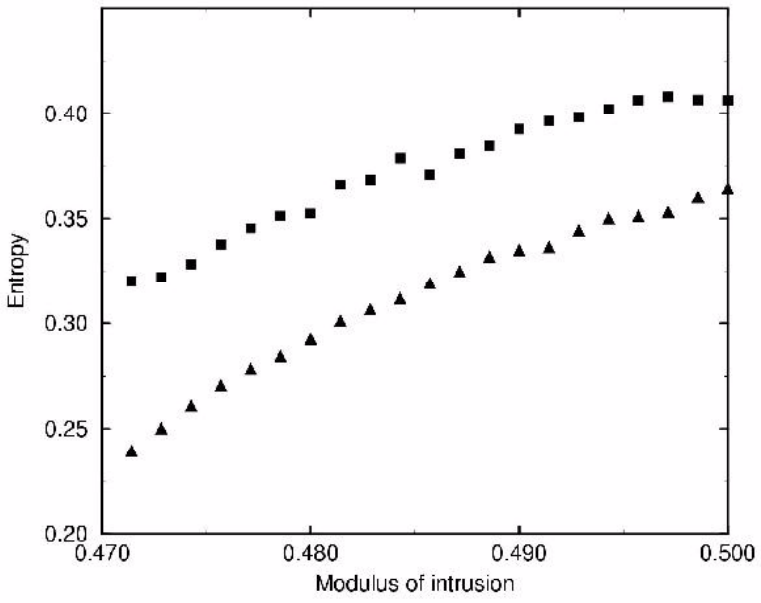

Figure 5. Same as in Figure 4, but dealing with entropies.

The largest differences $\Delta\rho$ and ΔS due to intrusion are observed for the aforementioned $\alpha = 45^o$. For $\alpha = 10^o$ and $\alpha = 85^o$, not shown in this paper, the differences are much less accentuated.

4.4 More on the random walker and other topics

The random walker of subsection 2.6 can be made to vary with space and with time. In order to show how versatile the manner in which the random walker is herein defined, we shall present two examples of deposition (see Figures 6 and 7). There is a random walker, # 1, which may choose any of the 5 possible directions; it is given by $D(I) = 1/5$, for $I = 1$ to 5. There is another random walker, # 2, which has the following properties: $D(1) = D(5) = 0.45$, $D(2) = D(4) = 0.05$, and $D(3) = 0$; this second walker may perform most of its steps, 90 %, in the two horizontal directions, and a few downwards and inclined steps. From what we have hitherto seen, it may be expected that random walker # 1 shall produce a dense object, while random walker #2 shall produce an object with a columnar structure of lower density. For both figures the lattices are composed of square cells, and the region of deposition has $J_F = 1000$ units wide; the height is $K_F = 1000$ units for Figure 6 and $K_F = 1800$ for Figure 7.

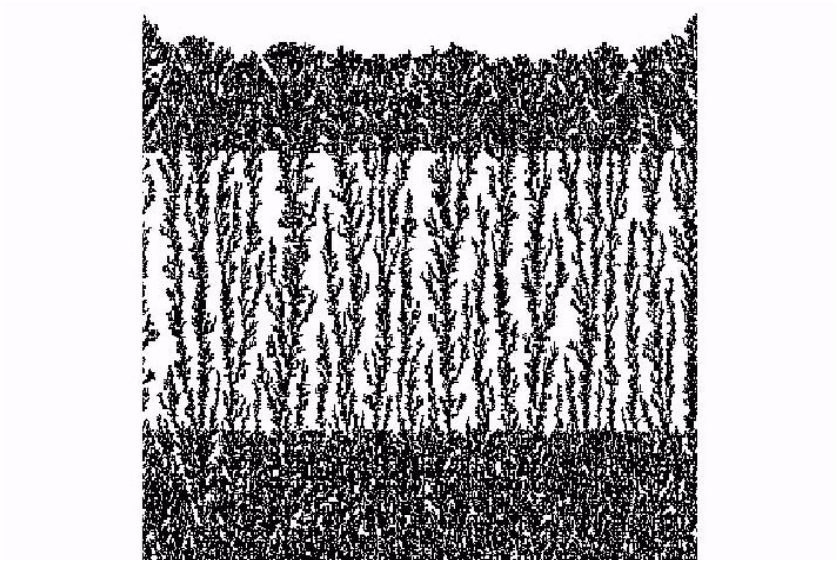

Figure 6. An object generated through deposition of particles by two different random walkers. The high density lower and upper layers are the result of random walker #1, with the possibilities given by $D(I) = 1/5$, for $I = 1$ to 5; the low density middle layer comes from random walker #2, with more chances to choose lateral steps: $D(1) = D(5) = 0.45$, $D(2) = D(4) = 0.05$, and $D(3) = 0$. The region of deposition is 1000 units wide by 1000 units high. See Figure 7 for comparison.

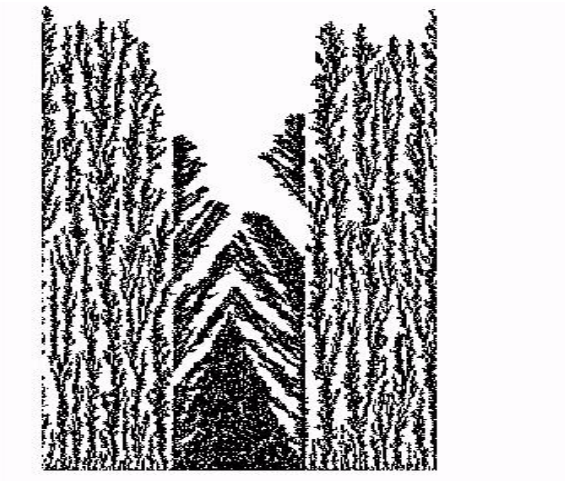

Figure 7. The same two walkers of Figure 6, but now random walker #1 acts on the vertical middle strip, while random walker #2 grows the object in the lateral strips. The region of deposition is 1000 units wide and 1800 units high. Though this object is quite different from the one of Figure 6, they have the same function relating areas and perimeters: $A = 0.579\,P$. The function is linear because the probabilities of changes of perimeter do not change with the area (in our case a measure of time); the slope of the function is the same because the probabilities of changes of perimeter are equal for both objects.

Figure 6 shows the result of the action of walker # 1 when the height, H, of the object is in the ranges, $1 \leq H \leq K_F/4$ and $3\,K_{F.}/4 \leq H \leq K_F$, while walker # 2 grows the object in the range $K_F/4 < H < 3\,K_F/4$. The high density upper and lower layers due to walker # 1, and the low density middle layer due to hesitating walker # 2, with its columnar structure, are clearly seen. The object has a maximum area, $A_{\max} = 249124$ units. Probabilities of changes of perimeter remain constant in the range, $A_{\max}/4 \leq A \leq A_{\max}$, with the following values: $p(-2) = 0.00688$, $p(0) = 0.12252$ and $p(+2) = 0.87060$. From Eqs. (3.5) and (3.11), or Eq. (4.2), the slope of the linear function, $A = f_f P$, is given by

$$f_f = \frac{\Delta A}{[-2p(-2) + 2p(+2)]} = \frac{1}{[-2 \times 0.00688 + 2 \times 0.87060]} = 0.57889$$

The entropy of the object is $S = 0.3752$.

We now turn our attention to the object shown in Figure 7, generated by the same two walkers, but now they act in two different vertical regions instead of horizontal layers. Walker # 1 deposits particles when the J column (the column where the walk starts, chosen at random), is in the middle range, $J_F/3 < J < 2\,J_F/3$; walker #2 has the lateral ranges of action, $1 < J \leq J_F/3$ and $2\,J_F/3 \leq J \leq J_F$. The final number of particles is $A_{\max} = 309854$; for the range of areas, $A_{\max}/4 \leq A \leq A_{\max}$, the probabilities of changes of perimeter are similar to the previous example: $p(-2) = 0.00776$, $p(0) = 0.12098$ and $p(+2) = 0.87126$; in consequence, the slope of the function is also similar

$$f_f = \frac{1}{[-2 \times 0.00776 + 2 \times 0.87126]} = 0.57904$$

This particular object shows that the columnar structure due to walker # 2 casts a shadow over the region where walker # 1 is acting, thus confining the region of high density. The entropy of this object is similar to the one of Figure 6: $S = 0.3762$.

Though the form of the objects shown in Figures 6 and 7 are quite different, the so called form factor, a name which seems to be misleading, is the same for both examples, i.e., areas and perimeters are governed by the same linear function. The slope of this function contains variables coming from the changes of perimeter and their respective probabilities.

The methods used in this paper have also been applied to other growth processes, such as diffusion-limited aggregation, with and without space and time variations of the random walker; the results seem to be encouraging. Nevertheless, the study of the Model of Eden, as the current literature shows, appears to be a special case, perhaps due to an endless transient state and, also, due to its high density; large areas and relatively low perimeters make the Model of Eden strongly dependent on randomness. The results of numerical experiments with multiple random walkers, and on other growth phenomena, are not herein presented because they go beyond the scope of this paper.

5 Conclusions

Deposition of particles depends on the probabilities of changes of perimeter each time a new particle is added to the cluster, and on the possibilities of a walker to perform random steps in explicit directions.

The function relating the area and its perimeter, for these objects with small areas and large perimeters (low densities), is linear. This property is due to the constancy of the probabilities of changes of perimeter. By theoretical means it is shown that the slope of the function depends on the sum of the products of the changes of perimeter by their respective probabilities.

Objects generated on a lattice composed of square cells are less dense and behave in a more disorderly fashion (higher entropy) than those generated with triangular cells.

There is a rather wide range of objects, produced with different types of random walkers, which result in a constant entropy and different densities.

References

[1] FAMILY, F. and VICSEK, T., editors, *Dynamics of fractal surfaces,* Word Scientific, 1991.

[2] MEAKIN, P., *Phys. Rev. Lett. A*, v. 33, p. 3371, 1986.

[3] MEAKIN, P., *Phys. Rev. Lett. B*, v. 30, p. 4207, 1984.

[4] WITTEN, T. A., and SANDER, L. M., *Phys. Rev. Lett.*, v. 47, p. 1400, 1981.

[5] ORR, C., editor, *Filtration Principles and Practices*, New York: Dekker, 1977.

[6] WEBER, W. J., *Physiochemical Processes for Water Quality Control*, New York: Wiley-Interscience.

[7] VOSSEN, J. L. and KERN, W., *Thin Film Processes*, New York: Academic, 1972.

[8] LEAMY, J. GILMER, G. W. and DIRKS, A. G., In: KALDIS, E. "*Currents Topics in Material Science*", v. 6, Amsterdam: North Holland, 1977.

[9] GILMER, G. W. and JACKSON, K. A., In: KALDIS, E., and SCHEEL, H.J. "*Com; puter Simulation of Crystal Growth*", Amsderdam: North Holland, 1977.

[10] TULLY, J. C., GILMER, G. W. and SCHUGARD, M., *J. Chem. Phys.*, v. 71, p. 1630, 1979.

[11] GILMER, G. W., *Science*, v. 208, p. 355, 1980.

[12] MEDALIA, A. J., *Surf. Colloid Sci.*, v. 4, p. 1, 1971.

[13] FRIEDLANDER, S. K., *Smoke, Dust and Haze*, New York: Wiley, 1977.

[14] MULLINS, W. W. and SEKERKA, R. F., *J. Appl. Phys.*, v. 34, p. 323, 1963.

[15] MCKENZIE, D. S., *Phys. Rep. C*, v. 21, p. 35, 1976.

[16] FLORY, P. J., Principles of Polymers Chemistry, Ithaca: Cornell University Press, 1979.

[17] GREENNES, P. G., *Scaling Concepts in Polymer Physics,* Ithaca: Cornell University Press, 1979.

[18] STANLEY. H. E., *J. Phys. A*, v. 10, p. 1-211, 1979.

[19] KIRKPATRIK, S., *Rev. Mod. Phys.*, v. 45, p. 547, 1973.

[20] PETERS, H., STAUFFER, D., HÖLTERS, H. P. and LOEWICH, K., *Z. Phys. B*, v. 34, p. 399, 1979.

[21] LEATH, P. L., *Phys. Rev. B*, v. 14, p. 5046, 1979.

[22] STAUFFER, D., *Phys. Rev. Lett.,* v. 41, p. 1333, 1978.

[23] STAUFFER, D., *Phys. Rep.,* v. 54, p. 3, 1979.

[24] ESSAM, J. W., *Rep. Prog. Phys.*, v. 43, p. 833, 1980.

[25] BOMB, C., SCHNEIDER, T., and STOLL, E., *J. Phys. A*, v. 8, L90-94, 1979.

[26] STANLEY, H. E., *Introduction to Phase Transitions and Critical Phenomena*, New York: Oxford Univ. Press, 1971.

[27] HERMANN, H. J., LANDAU, D. P. and STAUFFER, D., *Phys. Rev. Lett.*, v. 49, p. 419, 1981.

[28] KLEIN, W., *Phys. Rev. Lett.*, v. 47, p. 1559, 1981.

[29] FORREST, S. R. and WITTEN, T. A., Jr., *J. Phys. A*, v. 12, p. L109, 1979.

[30] WIEGEL, F. W. and PERELSON, A. S., *J. Stat. Phys.*, v. 29, p. 813, 1982.

[31] NIEMEYER, L., PIETRONERO, L. and WEISMANN, A. J., *Phys. Rev. Lett.*, v. 52, p. 1033, 1984.

[32] PATTERSON, L., *Phys. Rev. Lett.*, v. 52, p. 1621, 1984.

[33] BRADY, R. M. and BALL, R.C., *Nature*, v. 309, p. 225, 1984.

[34] MATSUSHITA, M., SAND, M., HAGAKAWA, Y. and SAWADA, Y., *Phys. Rev. Lett.*, v. 53, p. 386, 1984.

[35] MUTHUKUMAR, M., *Phys. Rev. Lett.*, v. 50, p. 839, 1983.

[36] GOULD, H., STANLEY, H. E. and FAMILY, F., *Phys. Rev. Lett.*, v. 50, p. 686, 1983.

[37] NAUENBERG, M., *Phys. Rev. B*, v. 28, p. 449, 1983.

[38] NAUENBERG, M., RICHTER, R. and SANDER, L. M., *Phys. Rev. B*, v. 28, p. 1649, 1983.

[39] DEUTCH, J. M. and MEAKIN, P., *J. Chem. Phys.*, v. 78, p. 2093, 1983.

[40] TOKUYAMA, H. and KAWASAKI, K., *Phys. Lett. A*, v. 100, p. 337, 1984.

[41] MEAKIN, P., *Phys. Rev. A*, v. 27, p. 495 and p. 604, 1983.

[42] RICHTER, R., SANDER, L. M. and CHENG, Z. M., *J. Colloid Interface Sci.*, v. 100, p. 203, 1984.

[43] MEAKIN, P., *Phys. Rev. Lett.,* v. 51, p. 1119, 1984.

[44] OLB, M., BOTET, R. and JULLIEN, R., *Phys. Rev. Lett.*, v. 51, p. 1123, 1983.

[45] WITTEN, T. A. and MEAKIN, P., *Phys. Rev. B,* v. 28, p. 5632, 1983.

[46] MEAKIN. P., *Phys. Rev. B*, v. 28, p. 5221, 1983.

[47] RÁCZ, Z. and VICSEK, T., *Phys. Rev. Lett.*, v. 51, p. 2382, 1983.

[48] JULLIEN, R., KOLB, M. and BOTET, R., *J. Phys.*, v. 45, p. 395, 1984.

[49] PIETRONERO, L. and TOSATTI, E. , eds.: "Fractals in Physics", Amsterdam: North Holland, 1986.

[50] FEDER, J., *Fractals*, New York: Plenum, 1988.

[51] MEAKIN, P., *Phase Transition and Critical Phenomena*, eds.: DOMB, C. and LEBOWITZ, J., v. 12, p. 355-484, New York: Academic, 1988.

[52] VICSEK, T., *Fractal Growth Phenomena*, Singapore: World Scientific, 1992.

[53] AHARONY, A. and FEDER, J., editors of *Fractal in Physics,* Amsterdam: North Holland, 1990.

[54] AHARONY, A. and FEDER, J., *J. Phys. D,* v. 38, p. 1-398, 1981.

[55] KAKUTANI, S., *Proc. Imper. Acad. Sci. (Tokio)*, v. 20, p. 706-714, 1944.

[56] EDEN, M., *Proceedings of the Fourth Berkeley Symposium on Mathematical Statistics and Probability,* v. IV, p. 223, Ed. NEYMAN, J., Berkeley: University of California Press, 1961.

[57] PARRY, W., *Entropy and Generator in Ergodic Theory*, New York: W. A. Benjamin, 1969.

[58] MANDELBROT, B. B., *The fractal geometry of Nature*, San Francisco: Freeman, 1982.

[59] CARUSO, H. A., *Revista Ciências Exatas e Naturais,* Ano 1, N^0 1, p. 9-22, 1999.

[60] CARPINTERO, D., *Boletín de la Asociación Argentina de Astronomía*, v. 36, p. 166, 1990.